PUBLISHED AS: Laura Galleni, Faegheh S. Sajjadian, Thierry Conard, Ivan Pollentier, Kevin M. Dorney, Fabian Holzmeier, Esben Witting Larsen, Daniel Escudero, Geoffrey Pourtois, Michiel J. van Setten, Paul van der Heide, John S. Petersen, "A scientific framework for establishing ultrafast molecular dynamic research in imec's AttoLab," Proc. SPIE 12498, Advances in Patterning Materials and Processes XL, 124980W (30 April 2023); https://doi.org/10.1117/12.2660047

A scientific framework for establishing ultrafast molecular dynamic research in imec's AttoLab

Laura Galleni[1,2 *], Faegheh S. Sajjadian[1,2], Thierry Conard[2], Ivan Pollentier[2], Kevin M. Dorney[2], Fabian Holzmeier[2], Esben Witting Larsen[2], Daniel Escudero[1], Geoffrey Pourtois[2], and Michiel J. van Setten[2, *], Paul van der Heide[2], John S. Petersen[2*]

1) Department of Chemistry, KU Leuven, Celestijnenlaan 200F, 3001 Leuven, Belgium
2) Imec, Kapeldreef 75, 3001 Leuven, Belgium

*E-mail: john.petersen@imec.be, laura.galleni@imec.be, michiel.vansetten@imec.be

Science stands on three legs: hypothesis, experiment, and simulation. This holds true for researching extreme ultraviolet (EUV) exposure of photoresist. Hypothesis: For resist exposure as patterns get smaller and closer together, approaching molecular units in width and resist-height, the molecular dynamics will limit the working resolution of the resist due to the formation of printing defects. Without taking proper consideration of these dynamics, the single-patterning lithography roadmap may end prematurely. Experimentally we are developing methods for sub-picosecond tracking of photoionization-induced processes. Using ultrashort pulses of light to excite and probe new materials with techniques that show the interactive dynamics of electronic and nuclear motion at the very limits of light-speed. This certainly holds true for exposing photoresists with EUV where ultrafast photoreactions induce chemical change via multiple pathways such as high-energy ionization fragmentation, recombination, and multispecies combination that ideally end in low-energy electron transfer reactions, analogous to lower energy photoreaction (but with a charge). In the nonideal case, these reaction processes lead to incompatible byproducts of the radiolysis that lead to types of stochastic defects. To do ultrafast studies we must build a foundation of knowledge using atomistic simulation to interpret transient molecular dynamic processes. Before we can do this, we need to learn how to simulate various spectral modalities to provide a starting point. In this work, we examine X-ray Photoelectron Spectroscopy of a model resist and use atomistic simulation to interpret the reactant-product composition of the spectral samples.

Introduction

We seek to better understand the ultrafast kinetics of the EUV radiolytic processes. Using ultrashort pulses of light to excite and probe new materials with techniques that show the interactive dynamics of electronic and nuclear motion at the very limits of light-speed is critical to the development and production of quantum age materials. This certainly holds true for 2D and topological materials that may be used to produce advanced-generation devices, but it also holds true for the primary topic of this paper, exposing photoresists with ionizing energy. Referring to Figure 1, in EUV exposure, ultrafast photoreactions induce chemical change via numerous pathways such as high-energy ionization fragmentation, recombination, and multispecies combination that ideally end in low-energy electron transfer reactions, forming reaction products analogous to lower energy, deep UV (DUV), photoreactions shown by the lower dose post developmetn resist thickness.[1,2] In the nonideal case, other reaction processes lead to incompatible byproducts of the radiolysis via cross-linking free-radical polymer fragments[3, 4] shown in the higher dose region to form insoluble products that lead to nanobridge/missing via defects and, speculating, other yet unidentified products that lead to highly soluble defects leading to nanobreaks/connecting (kissing) vias. These radiolytic processes are ultrafast with the cascading secondary electrons from ~80 eV to below 10 eV completing in less than a picosecond.[5] Without taking proper consideration of these dynamics and fixing them, the end of the single-patterning lithography production resolution roadmap maybe premature.

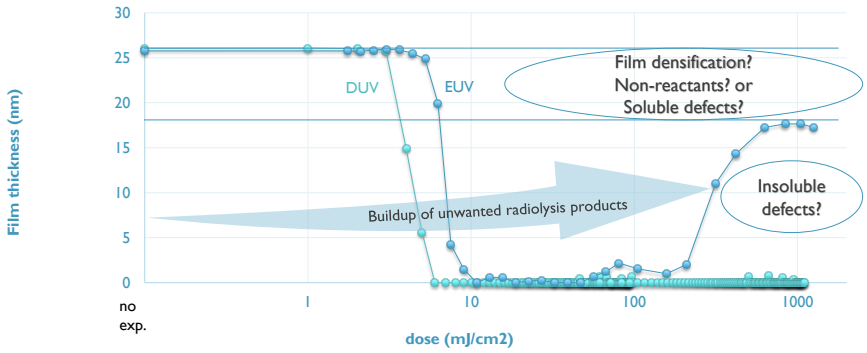

Figure 1: Two photoresist contrast curves; one from exposure to DUV and the other with EUV[1]. The EUV curve leads to a tonal flip at high dose with buildup of unwanted radiolytic products. Hypothesis: Unwanted radiolysis pathways lead to some types of stochastic defects.

With this in mind, in 2019 imec announced plans at SPIE Advanced Lithography to build the AttoLab with joint development partners KMLabs and SPECS.[6, 7] This lab is the first industrial laboratory attempting the real time, *in-situ* observation of radiolytic kinetics of EUV resist exposure and ultimately aims to detect the ultrafast (short-lived) molecular transients following exposure to 13.5 nm radiation with a tabletop EUV source.

As of the writing of this paper in February 2023, development of capabilities for EUV reflectometry and radiometry characterization[8] and steady-state angle-resolved photoemission spectroscopy[9] on conducting materials is complete, and the capabilities are open for research. The schematic of the laboratory is described in more detail in Figure 2.[10]

What remains is the ability to experimentally study the chemical kinetics and excited state transients of these complex resist systems during EUV exposure with the intent to engineer

Figure 2: Layout of the imec-AttoLab laboratory, and ultrafast nanoscale metrology and high-NA EUV lithography lab. The lab is centered around two tabletop EUV systems based on high-harmonic generation, which supply coherent EUV light for spectroscopy, imaging, inspection, ARPES, PEEM, and lithography experiments at a variety of endstations.

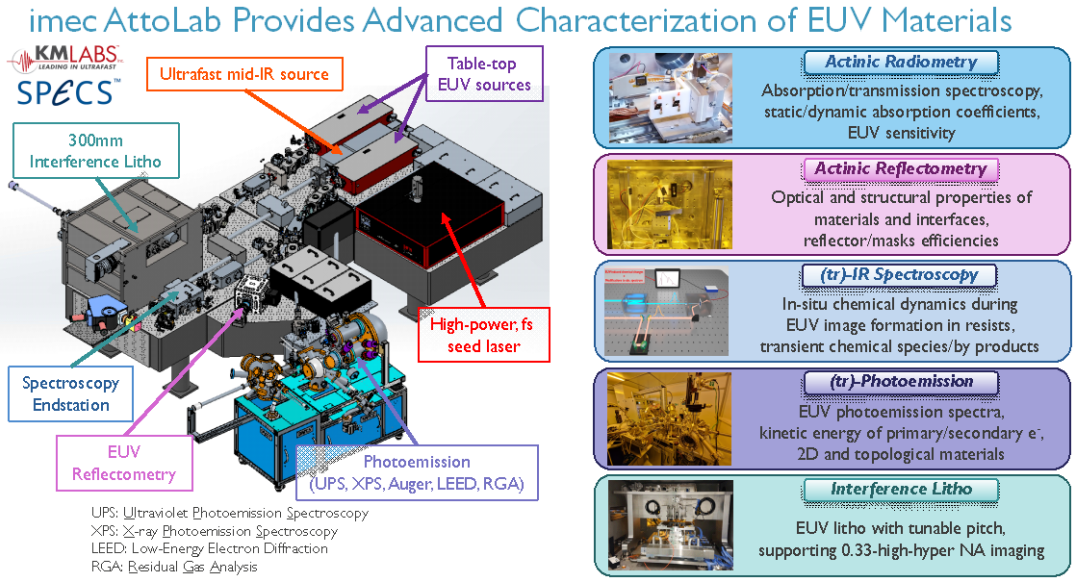

new higher performance materials. Understanding, identifying, and interpreting transient species in resist during exposure to EUV radiation is nontrivial. To accomplish we will need to stand on the three pillars of modern science: Hypothesis, Experiment, and Simulation. Our hypothesis states that ultrafast radiolysis is made of many reaction pathways and that some lead to desirable reactions compatible with later processing and others do not, leading to stochastic print failures. Experimentally we plan ultrafast pump-probe spectroscopy to detect transients to map the radiolytic pathways and then leverage atomistic and molecular dynamics simulations to interpret the resulting spectroscopic signatures. To get this far requires upfront experimental and additional simulation work to characterize reactants and products. We use EUV radiometry and reflectometry, Fourier-transform infrared (FTIR) spectroscopy and recently studies of resist-primitives using photo excitation photo ionization coincidence (PEPICO) spectroscopy[11] to aid in constructing a picture of the resist structure and changes in the resist triggered by EUV exposure.

Among other useful techniques, photoemission is essential as it allows direct probing of chemical bonds in a quantitative way by providing the energy and abundance of the generated photoelectrons upon EUV exposure.[12] However, since high-energy photons are being employed for characterization of a photosensitive material, modification of the sample (e.g., activation of the photoacid generator (PAG) and production of radiolytic products) during the measurement occurs and must be considered when investigating the chemical changes in the photoresist before and after exposure to EUV light.

In this research, we investigate the chemical changes occurring during the photoemission measurements of an unexposed, model chemically amplified resist (CAR) using X-rays photoemission (Al Kα 1486.6 eV) based on the well-known environmentally stable chemically amplified photoresist (ESCAP, an environmentally stable CAR)[26] as a function of several measurement parameters such as X-ray photon density and the use of a charge neutralization system. Atomic force microscopy (AFM) and x-ray photoemission spectroscopy (XPS) elemental mapping are employed to interpret the nature of the chemical modifications detected after XPS measurement. We then use first principles atomistic simulations to interpret the experimental results.[23]

Experimental Method

A model ESCAP material consisting of a poly [(t-butyl methacrylate)-co-(p-hydroxystyrene)] copolymer (PBMA-PHS), mixed with a PAG, a quencher molecule, and two residual solvents, together with samples of its polymer component (without PAG and quencher) were used for XPS measurements.[26]

XPS measurements were performed on either a VersaProbe III instrument or a Quantes instrument, both from Ulvac-PHI, using a monochromatized Al K_α (1486.6 eV) photon beam. All measurements were recorded at an exit angle of 45°. The effect of the X-ray beam on the chemical analysis was investigated using the VersaProbe instrument by varying the X-ray photon density by modifying the total measurement time from 9 to 115 minutes with a 100 μm spot and/or by rastering the X-ray beam over an area of 1000×500 μm^2. The visualization of the chemical changes was performed using elemental mapping by XPS in the Quantes instrument with a 20 μm spot over an area of 500 ×500 μm^2.The samples were kept in the vacuum chamber for approximately 18 hours before the measurements to ensure that all material outgassing was complete and that the vacuum level in the chamber was sufficiently low (below 10^{-7} Pa) to carry out XPS. A Tougaard background[13,14] was computed with CasaXPS[15] and subtracted from the raw data.

The AFM system r-ICON PT, Nanoscope V was used to observe changes in morphologies of samples.

Computational Method

All calculations were performed using Turbomole 7.2[16]. Atomic structures were optimized in vacuum with density functional theory (DFT) using the Perdew-Burke-Ernzerhof (PBE) functional[17] and a Gaussian basis set of triple-ζ valence quality (def2-TZVP)[18]. Carbon 1s core-level binding energies of each molecule were calculated with single-shot *GW* (G_0W_0).[19] As a starting point for G_0W_0, Kohn-Sham orbitals and eigenvalues were obtained from DFT using the BH-LYP functional[20, 21, 22] and a Gaussian basis set of split valence quality (def2-SVP) combined with resolution of identity18. The functional and basis set were chosen according to a previous benchmark.[23] A Gaussian broadening of 0.6 eV was applied to each binding energy. The spectra of all building blocks were summed up, weighted by the nominal molar ratios.[23] A rigid shift of 7.33 eV was applied to all binding energies to align the main C 1s peak at 284.8 eV.

Results and Discussion

The model ESCAP material's C 1s, O 1s, F 1s and S 2p XPS data were measured and the nominal molar ratio of each component is reported in Figure 5. The resist was not previously exposed to EUV.

XPS measurements were performed on one point of a sample of 2×3 cm^2 of the model resist for 60 minutes. After the XPS measurements, a post exposure bake (PEB) and resist-development procedure were applied in order to visualize the damaged area in an optical microscope. It showed that the XPS measurement spots of a few hundreds of squared micrometers large are easily revealed, as shown in Figure 3. Since the ESCAP formula is too complicated to allow a direct interpretation of the spectra, reference XPS measurements with the same conditions were performed on a sample of the polymer component (without PAG and quencher). In that case, no damages were observed neither from the spectra nor under the optical microscope after PEB and development. It appears thus that the damage arises from the activation of PAG and/or quencher. This was further confirmed from electronic structure calculation.

To interpret the optical image, two different measurements were performed. First, AFM was carried out on an area covering the non-exposed resist outside of the exposed spot up to the middle of the damage spot after 60 min XPS measurement as shown in Figure 3. AFM measurement shows the presence of full resist in the non-exposed area (80 to 60 µm, height of ~0) followed by a completely developed area (60 to 40 µm, height of ~-35 nm corresponding to the thickness of the photoresist layer), which goes towards the center area that seems not to be fully developed (40 to 0 µm, with a maximum resist height of ~-20 nm).

Second, since AFM does not provide any elemental information, an XPS elemental mapping of the Si and C intensities was performed on the same damage spot. As observed in Figure 4, Si substrate is clearly detected in the area where it was expected to be fully developed due to AFM measurement. The low concentration of carbon detected in this area and the high concentration on the non-exposed resist area could be attributed to the presence of carbon contamination and the polymer backbone in the non-exposed ESCAP, respectively. This observation shows similarities with the dose-to-clear diagram of an over-exposed EUV-resist to EUV light (Figure 1 where thickness increases in the high dose range and then appears to reverse again at the highest dose.) and is consistent with the fact that a higher x-ray photon

density is present at the center of the x-ray beam. However, more investigation is needed to understand the full effect of the interaction of x-ray from XPS measurements and resulting chemical modifications.

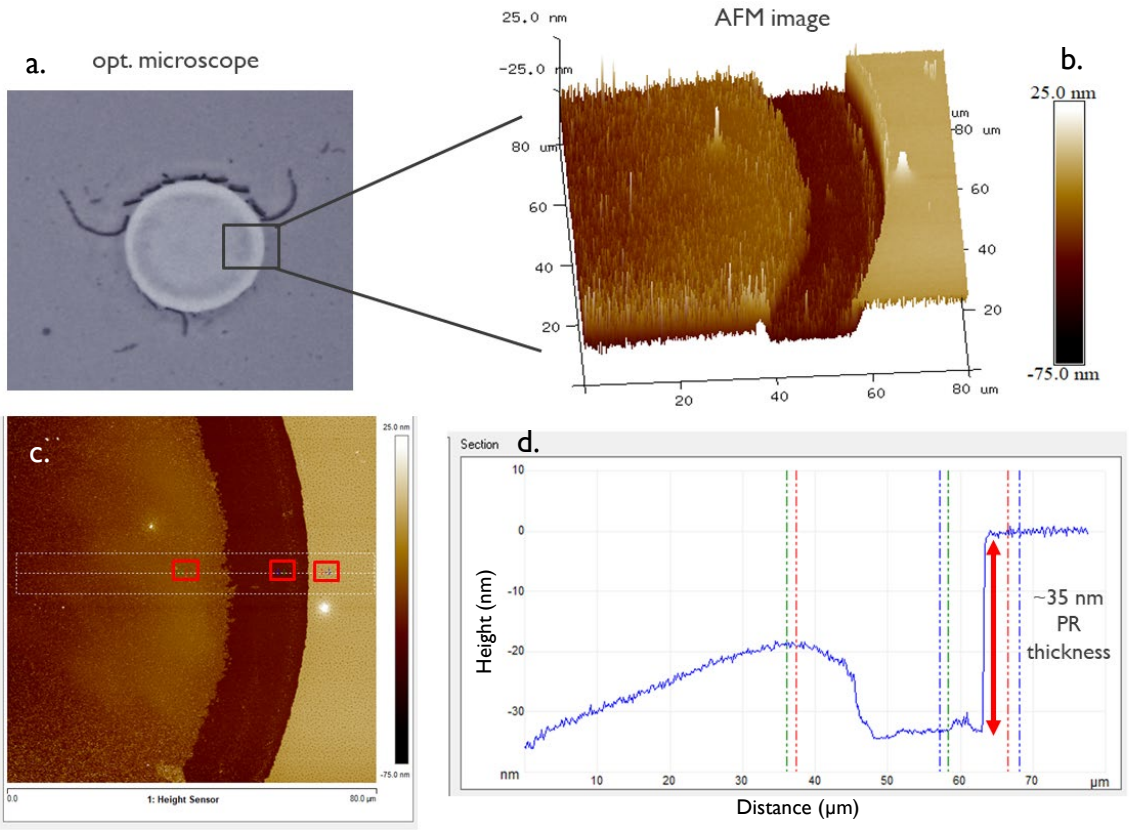

Figure 3: Damage spots after 60 min XPS measurement, PEB and development under optical microscope (a.) and AFM results on the same spot (b. 3D image; c. 2D image; d. The graph of height vs distance for the scanned AFM area).

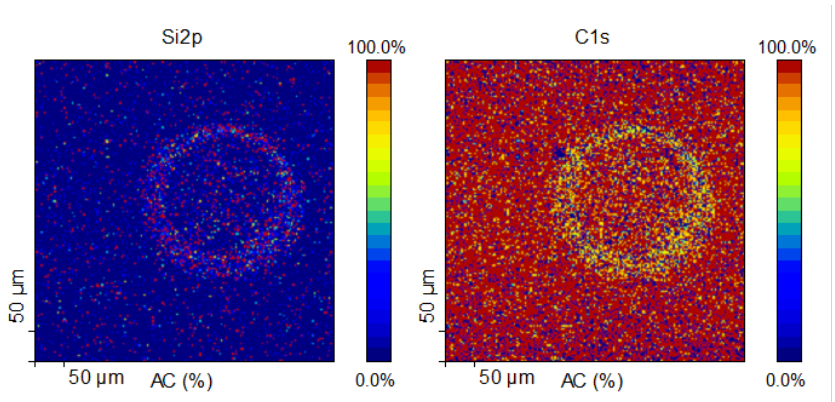

Figure 4: XPS elemental mapping on the damage spot after 60 min XPS measurement, PEB and development Left is the Si2p and the right C1s.

These results show that to use XPS for analyzing EUV-resist interactions it is necessary to develop a measurement protocol to avoid measurement-induced modification. In our settings, we determined that the best way is to measure the sample for a limited time that still satisfies the signal-to-noise (SNR) ratio (45 min for this sample), without neutralization system and

using a large raster for the x-ray spot (1000×500 μm^2). These results will be reported elsewhere.

To interpret the experimental data, we simulate the XPS spectrum of the resist using state-of-the-art first-principles calculations. More specifically, we use the methodology reported in ref. 25 in which we make the computational cost manageable by approximating the ESCAP as a collection of isolated building blocks, corresponding to the molecules shown on top of Figure 5. Instead of the PBMA-PHS copolymer, we separately consider the two isolated monomers of PBMA and PHS in vacuum, capped with hydrogen atoms.[25] For each building block, we simulate the C 1s XPS spectrum by applying a Gaussian broadening to the binding energies calculated in vacuum from single-shot *GW* (G_0W_0) calculations on top of DFT at the BH-LYP/def2-SVP level of theory (G_0W_0@BH-LYP/def2-SVP). The spectra of all building blocks are then summed up, weighted by their nominal molar ratio to simulate the spectrum of the full CAR. The resulting spectrum is then shifted to match the main carbon peak at 284.8 eV and compared with the experiment.

Figure 5a shows the simulated spectrum of the unexposed resist. A discrepancy can be observed between the theoretical and measured peak around 288.5 eV. This peak results from the overlap of the C=O peaks in PBMA and Solvent 1 and the C–S peaks in PAG^- (nonaflate anion) and PAG^+ ((4-Methylphenyl) diphenyl sulfonium cation). However, the latter is the most significant contribution. The discrepancy might thus arise from the reaction of PAG^+.

To investigate this further, we simulate the spectrum of the same resist after replacing the unreacted PAG^+ with the products of a photodissociation reaction. As a first guess, we consider the photodissociation pathways of triphenylsulfonium[24],[25], which differs from our PAG^+ by only one methyl group. Upon exposure to UV light, the triphenylsulfonium is known to form (i) diphenyl sulfide or (ii) (phenylthio)biphenyl isomers.[24, 25] Therefore, for our simulation we consider these two photoreactions, with the addition of a methyl group to the products, as shown in Figure 5b and 5c. The calculated XPS C 1s peaks of the products of both photoreactions are largely overlapping, with a relative shift of only 0.2 eV (Figure 6). Interestingly, the calculated XPS C 1s peak for the photoproducts are shifted by 3.6 and 3.8 eV from the peak of the unreacted PAG^+, respectively (Figure 6). The photodissociation of PAG^+ can therefore be detected experimentally.

The theoretical XPS spectrum for the full ESCAP after photodissociation of PAG^+ is reported in Figure 5b and 5c. The agreement between the simulated spectrum and the experimental data improves significantly if we assume that the PAG^+ has undergone photodissociation. This is not surprising, as the photodissociation is expected to occur upon exposure to UV light and the resist under study was exposed to x-rays during the XPS measurement. This suggests that the XPS measurement is activating the photoresist.

Conclusions

To begin the journey to studying the transient kinetics of radiolytic processes, we develop simulations that interpret our current spectral analysis. Here we present steady state XPS photoemission spectra of a model resist and show the power to interpret our spectra using simulation.[26]

Experimentally, we demonstrate that the loss of thickness in the exposure regime of the tonal reversal in Figure 1 is visually not apparent after PEB suggesting that is not densification and

is apparent only after development but remains the subject of future investigation to determine if it is just deprotected uncross-linked polymer or some new moiety. We do show in that dose region that chemical changes are understood through theoretical modelling of X-ray photoemission spectra.23 Based on these results, we propose a measurement protocol allowing to minimize or eliminate this modification. This measurement protocol will help to guide (or enable) photoemission measurements on light-sensitive materials (photoresists) that result in minimal perturbation of the material itself, thus allowing for the observation of chemical changes that are directly resulting from DUV/EUV lithography process (i.e., exposure, pre/post exposure bake, etc.).

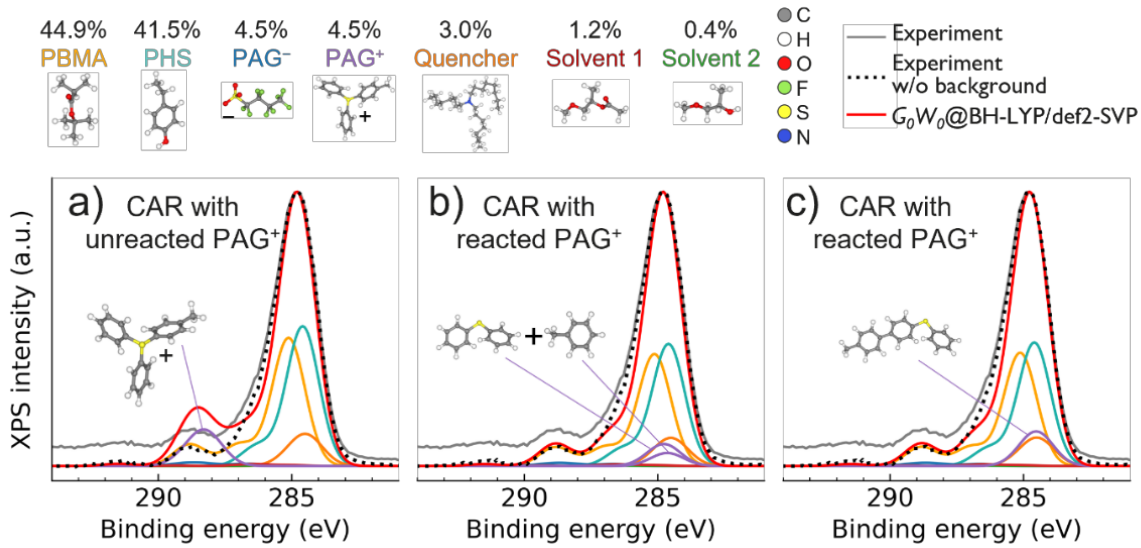

Figure 5: Normalized theoretical and experimental C 1s XPS spectra of a model chemically-amplified resist (ESCAP) consisting of a poly[(*t*-butyl methacrylate)-*co*-(*p*-hydroxystyrene)] copolymer (PBMA–PHS), mixed with a photoacid generator (PAG), a quencher molecule, and two residual solvents. The simulated spectrum was calculated assuming (a) unreacted or (b, c) reacted PAG^+. Spectra b and c show the best agreement with the experiment.

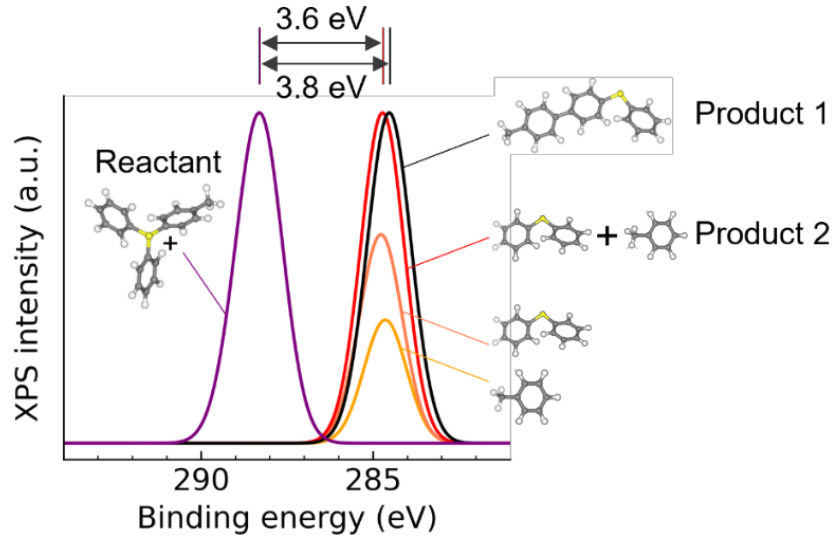

Figure 6: Normalized theoretical C 1s XPS spectra of the unreacted PAG^+ and its photoproducts calculated with G_0W_0@BH-LYP/def2-SVP.

To close, the potential of AttoLab lies in our ability for garnering information about the dynamics of quantum systems that cannot be gained otherwise through steady-state energy-domain measurements and then relating them to lithographic results for resists and quantum age devices. Combining coherent control, attosecond EUV pulses, and powerful spectroscopic and imaging techniques allows us to unravel mysteries, the miracles, of these systems. Combined with computational chemistry it permits us to probe our most profound physics theories, provides a systematic approach to understand and control ionization chemical reaction pathways, and could ultimately advance material development in many areas of endeavor (resists and beyond). [27]

Acknowledgement

The research leading to these results was enabled by funding from the European Union's Horizon 2020 research and innovation programme under the Marie Sklodowska-Curie grant agreement No.'s 101031245 (K.M.D.) and 101032241 (D.P.S.). We also graciously acknowledge Fuji Film for providing the model ESCAP material used in this work.

---

[1] I. Pollentier, Y. Vesters, J. S. Petersen, P. Vanelderen, A. Rathore, D. De Simone, G. Vandenberghe, "Unraveling the role of photons and electrons upon their chemical interaction with photoresist during EUV exposure," Proc. SPIE 10586, Advances in Patterning Materials and Processes XXXV, 105860C (19 March 2018).

[2] T. Kozawa and S. Tagawa, "Radiation Chemistry in Chemically Amplified Resists," Japanese Journal of Applied Physics, vol. 49, no. 3, p. 030001, Mar. 2010.

[3] D. J. T. Hill and A. K. Whittaker, "Radiation chemistry of polymers," in Encyclopedia of Polymer Science and Technology. New York: Wiley, 2004.

[4] H-H Cheng, A. Yu, I. Keen, Y. Chuang, K. S. Jack, M. J. Leeson, T. R. Younkin, I. Blakey, and A. K. Whittaker, Electron-beam induced freezing of an aromatic based EUV resist: a robust template for directed self assembly of block copolymers. IEEE Transactions on Nanotechnology 11 (6) 6293902 1140-1147 (2012).

[5] T. Kozawaa, T. Shigaki, K. Okamoto, A. Saeki, and S. Tagawa, "Analysis of acid yield generated in chemically amplified electron beam resist", J. of Vac. Science & Tech. B: Microelectronics and Nanometer Structures Processing, Measurement, and Phenomena 24, 3055 (2006).

[6] J. S. Petersen, "Then a miracle occurs: A description of the issues of EUV radiolysis process and the relationship to stochastic print failures (Conference Presentation)," Proc. SPIE 10960, Advances in Patterning Materials and Processes XXXVI, 1096006 (25 March 2019) (presentation).

[7] F. Holzmeier, K. Dorney, E. W. Larsen, T. Nuytten, D. P. Singh, M. van Setten, P. Vanelderen, C. Bargsten, S. L. Cousin, D. Raymondson, E. Rinard, R. Ward, H. Kapteyn, S. Böttcher, O. Dyachenko, R. Kremzow, M. Wietstruk, G. Pourtois, P. van der Heide, J. Petersen, "Introduction to imec's AttoLab for ultrafast kinetics of EUV exposure processes and ultra-small pitch lithography," Proc. SPIE 11610, Novel Patterning Technologies 2021, 1161010 (22 February 2021).

[8] K. Dorney, N. N. Kissoon, F. Holzmeier, E. W. Larsen, D. P. Singh, S. Arvind, S. Santra, R. Fallica, I. Makhotkin, V. Philipsen, S. De Gendt, C. Fleischmann, P. A. W. van der Heide, J. S. Petersen, "Actinic inspection of the EUV optical parameters of lithographic materials with lab-based radiometry and reflectometry", SPIE Adv. Litho.: Metrology, Inspection, and Process Control XXXVII, Paper 12494-62 (2023).

[9] D. P. Singh work in preparation.

[10] F. Holzmeier, K. Dorney, E. W. Larsen, T. Nuytten, D. P. Singh, M. van Setten, P. Vanelderen, C. Bargsten, S. L. Cousin, D. Raymondson, E. Rinard, R. Ward, H. Kapteyn, S. Böttcher, O. Dyachenko, R. Kremzow, M. Wietstruk, G. Pourtois, P. van der Heide, J. Petersen, "Introduction to imec's AttoLab for ultrafast kinetics of EUV exposure processes and ultra-small pitch lithography," Proc. SPIE 11610, Novel Patterning Technologies 2021, 1161010 (22 February 2021).

[11] F. Holzmeier, M. Gentile, M. Gerlach, R. Richter, M. J. van Setten, J. S. Petersen, P. A. W. van der Heide, "Dissociative photoionization of EUV lithography photoresist models", Paper 12498-26

[12] O. Kostko, et al., Proc. SPIE 11854, International Conference on Extreme Ultraviolet Lithography 2021, 1185407 (2021).

[13] M. H. Engelhard, D. R. Baer, A. Herrera-Gomez, and P. M. A. Sherwood, "Introductory guide to backgrounds in XPS spectra and their impact on determining peak intensities," J. Vac. Sci. Technol. A 38(6), 063203 (2020).

[14] S. Tougaard, and P. Sigmund, "Elastic and inelastic scattering of electrons emitted from solids: effects on energy spectra and depth profiling in xps/aes," Surf. Interface Anal. 9(2), 130–130 (1986).
[15] N. Fairley, V. Fernandez, M. Richard-Plouet, C. Guillot-Deudon, J. Walton, E. Smith, D. Flahaut, M. Greiner, M. Biesinger, S. Tougaard, D. Morgan, and J. Baltrusaitis, "Systematic and collaborative approach to problem solving using X-ray photoelectron spectroscopy," Appl. Surf. Sci. Adv. 5, 100112 (2021).
[16] "TURBOMOLE, V7.2, 2017, a development of University of Karlsruhe and Forschungszentrum Karlsruhe GmbH, 1989−2007, TURBOMOLE GmbH, since 2007; available from http://www.turbomole.com."
[17] J. P. Perdew, K. Burke and M. Ernzerhof, "Generalized Gradient Approximation Made Simple," Phys. Rev. Lett. 77(18), 3865–3868 (1996).
[18] F. Weigend and R. Ahlrichs, "Balanced basis sets of split valence, triple zeta valence and quadruple zeta valence quality for H to Rn: Design and assessment of accuracy," Phys. Chem. Chem. Phys. 7(18), 3297 (2005. 3).
[19] M. J. van Setten, F. Weigend, and F. Evers, "The GW-method for quantum chemistry applications: Theory and implementation," J. Chem. Theory Comput. 9(1), 232–246 (2013).
[20] A. D. Becke, "Density-functional exchange-energy approximation with correct asymptotic behavior," Phys. Rev. A 38(6), 3098–3100 (1988).
[21] Lee, C., Yang, W. and Parr, R. G., "Development of the Colle-Salvetti correlation-energy formula into a functional of the electron density," Phys. Rev. B 37(2), 785 (1988).
[22] A. D. Becke, "A new mixing of Hartree--Fock and local density-functional theories," J. Chem. Phys. 98(2), 1372–1377 (1993).
[23] L. Galleni, F. S. Sajjadian, T. Conard, D. Escudero, G. Pourtois, and M. J. van Setten, "Modeling X-ray Photoelectron Spectroscopy of Macromolecules Using GW," J. Phys. Chem. Lett. 13, 8666–8672 (2022).
[24] S. Tagawa, S. Nagahara, T. Iwamoto, M. Wakita, T. Kozawa, Y. Yamamoto, D. Werst, and A. D. Trifunac, "Radiation and photochemistry of onium salt acid generators in chemically amplified resists," Adv. Resist Technol. Process. XVII 3999(June 2000), 204 (2000).
[25] E. Despagnet-Ayoub, W. W. Kramer, W. Satter, A. Sattler, P. J. LaBeaume, J. W. Thackeray, J. F. Cameron, T. Cardolaccia, A. A. Rachford, J. R. Winkler, and H. B. Gray, "Triphenylsulfonium topophotochemistry," Photochem. Photobiol. Sci. 17(1), 27–34 (2018).
[26] Courtesy of Fuji Film Electronic Materials (FFEM).
[27] Paraphrased from Jens Biegert, ICFO